ISSN 1674-1056
http://cpb.iphy.ac.cn
http://iopscience.iop.org/cpb
中国物理 B
Chinese Physics
中国物理 Chinese Physics B

Hard carbons derived from pine nut shells as anode materials for Na-ion batteries

Hao Guo(郭浩), Kai Sun(孙凯), Yaxiang Lu(陆雅翔), Hongliang Wang(王洪亮), Xiaobai Ma(马小柏), Zhengyao Li(李正耀), Yong-Sheng Hu(胡勇胜), Dongfeng Chen(陈东风)

Citation: Chin. Phys. B . 2019, 28(6): 068203. **doi:** 10.1088/1674-1056/28/6/068203
Journal homepage: http://cpb.iphy.ac.cn; http://iopscience.iop.org/cpb

What follows is a list of articles you may be interested in

Influences of carbon coating on the electrochemical performance of SiO@C/graphite composite anode materials

Hao Lu(陆浩), Junyang Wang(汪君洋), Bonan Liu(刘柏男), Geng Chu(褚赓), Ge Zhou(周格), Fei Luo(罗飞), Jieyun Zheng(郑杰允), Xiqian Yu(禹习谦), Hong Li(李泓)

Chin. Phys. B . 2019, 28(6): 068201. **doi:** 10.1088/1674-1056/28/6/068201

Performance of n-type silicon/silver composite anode material in lithium ion batteries: A study on effect of work function matching degree

Guo-Jun Xu(徐国军), Chen-Xin Jin(金晨鑫), Kai-Jie Kong(孔凯捷), Xi-Xi Yang(杨西西), Zhi-Hao Yue(岳之浩), Xiao-Min Li(李晓敏), Fu-Gen Sun(孙福根), Hai-Bin Huang(黄海宾), Lang Zhou(周浪)

Chin. Phys. B . 2018, 27(10): 108201. **doi:** 10.1088/1674-1056/27/10/108201

Size effect of Si particles on the electrochemical performances of Si/C composite anodes

Bonan Liu(刘柏男), Hao Lu(陆浩), Geng Chu(褚赓), Fei Luo(罗飞), Jieyun Zheng(郑杰允), Shimou Chen(陈仕谋), Hong Li(李泓)

Chin. Phys. B . 2018, 27(8): 088201. **doi:** 10.1088/1674-1056/27/8/088201

Gas treatment protection of metallic lithium anode

Wen-jun Li(李文俊), Quan Li(李泉), Jie Huang(黄杰), Jia-yue Peng(彭佳悦), Geng Chu(褚赓), Ya-xiang Lu(陆雅翔), Jie-yun Zheng(郑杰允), Hong Li(李泓)

Chin. Phys. B . 2017, 26(8): 088202. **doi:** 10.1088/1674-1056/26/8/088202

RAPID COMMUNICATION

Hard carbons derived from pine nut shells as anode materials for Na-ion batteries*

Hao Guo(郭浩)[1], Kai Sun(孙凯)[1,†], Yaxiang Lu(陆雅翔)[2,3,‡], Hongliang Wang(王洪亮)[1], Xiaobai Ma(马小柏)[1], Zhengyao Li(李正耀)[1], Yong-Sheng Hu(胡勇胜)[2,3], and Dongfeng Chen(陈东风)[1,§]

[1] *China Institute of Atomic Energy, Beijing* 102413, *China*

[2] *Key Laboratory for Renewable Energy, Beijing Key Laboratory for New Energy Materials and Devices, Beijing National Laboratory for Condensed Matter Physics, Institute of Physics, Chinese Academy of Sciences, Beijing* 100190, *China*

[3] *School of Physical Sciences, University of Chinese Academy of Sciences, Beijing* 100190, *China*

(Received 27 March 2019; revised manuscript received 7 April 2019; published online 8 May 2019)

Hard carbons as promising anode materials for Na-ion batteries (NIBs) have captured extensive attention because of their low operation voltage, easy synthesis process, and competitive specific capacity. However, there are still several disadvantages, such as high cost and low initial coulombic efficiency, which limit their large-scale commercial applications. Herein, pine nut shells (PNSs), a low-cost biomass waste, are used as precursors to prepare hard carbon materials. Via a series of washing and heat treatment procedures, a pine nut shell hard carbon (PNSHC)-1400 sample has been obtained and delivers a reversible capacity of around 300 mAh/g, a high initial coulombic efficiency of 84%, and good cycling performance. These excellent Na storage properties indicate that PNSHC is one of the most promising candidates of hard carbon anodes for NIBs.

Keywords: Na-ion battery, anode, hard carbon, pine nut shells

PACS: 82.47.Cb, 82.45.Fk, 84.60.–h **DOI:** 10.1088/1674-1056/28/6/068203

1. Introduction

Li-ion batteries (LIBs), as the most successful energy storage technology, have been widely used in electronic devices and electric vehicles due to the high energy density, high power density, and environmental friendliness.[1–3] However, the increasing cost and resource shortage of lithium reserves may hinder their sustainable application in the future. The greater abundance and accessibility of Na have promoted the study and development of Na-ion batteries (NIBs), making them one of the most promising supplements to LIBs in large-scale stationary applications.[4–6] Generally, the research of NIBs can draw on the successful experience of LIBs because Na has the similar chemical and electrochemical properties to those of Li. Cathode materials, mainly including oxides, polyanionic compounds, *etc*.,[7–15] deliver the encouraging electrochemical properties in practical applications. However, graphite, which is widely used as anode materials for LIBs, exhibits limited Na storage capability due to the thermodynamic reasons.[16,17] Although it has recently shown that this limitation can be partially resolved using the expanded graphite[18] or ether-based electrolyte,[19] searching for the other anode materials, such as carbonaceous materials,[20–37] alloys,[38–40] oxides,[41–45] and organic compounds,[46] has attracted a wide range of attention to meet the requirements of higher Na storage capacity, excellent cycle/rate performance, and so on. Hard carbons (HCs), an amorphous carbon comprising random stacking graphene sheets, nanopores, and defects, have been regarded as one of the potential anodes for NIBs due to their good performance. Reversible Na insertion and extraction in hard carbons was first demonstrated by Dahn *et al.* in 2000.[20,21] Since then, many research groups have devoted considerable effort to improve their storage capacity and cycle/rate properties. On the one hand, numerous HCs derived from different precursors under optimal conditions, such as glucose,[20] anthracite,[22] pitch,[23] cotton,[24] and biomass wastes,[25–27] have been proposed to use as anodes for NIBs. On the other hand, many synthetic methods, such as pre-oxidation,[28] heteroatoms doping,[29,30] and nano technology,[31–33] have been developed to improve storage performance and kinetics of HCs. However, most of them show low initial coulombic efficiency and low reversible capacity, which cannot satisfy the requirements for practical applications. Xu *et al.* prepared hard carbons derived from pistachio shells by hydrothermal treatment at low temperature and carbonization at high temperature. The obtained anode delivers a high charge capacity of 317 mAh/g; however, the initial cycle efficiency is only 62%.[26] Sun *et al.* reported the facile

*Project supported by the President Fund Project of China Institute of Atomic Energy.

†Corresponding author. E-mail: ksun@sina.com

‡Corresponding author. E-mail: yxlu@iphy.ac.cn

§Corresponding author. E-mail: dfchenciae@126.com

© 2019 Chinese Physical Society and IOP Publishing Ltd

synthesis of hard carbon by one-step pyrolysis of shaddock peel.[27] The pyrolytic carbon shows very high reversible Na storage capacity up to 430 mAh/g. Nevertheless, the low initial cycle efficiency of 67% needs to be further improved. Commonly, the initial coulombic efficiencies of HCs derived from biomass wastes are often lower than 80%, which leaves more space to address this challenge in HC anodes.

How to understand the fundamental Na storage mechanism of HCs is also an important issue. Although many understandings have been achieved based on different characterization methods, controversial voices still exist.[21,34–36] Typically, the typical curve of Na storage in HCs shows two distinct regions: one slope above 0.1 V and one plateau below 0.1 V. The slope region has been attributed to either Na insertion into graphitic layers[21] or Na absorption at defects.[34,36] Similarly, the plateau region has been explained by either the Na intercalation between disordered graphite layers[34] or nanopore filling.[21,36] Several research groups consider that the plateau region is related to both Na intercalation and nanopore filling/plating.[35] Evidently, these different storage mechanisms result from the variation in the microstructure which depends on both the carbon precursor and thermal processing methods. Therefore, the correlation between the microstructure and charge-discharge behavior requires to be further studied, which can help to tailor the microstructure of carbon materials, leading to the enhanced electrochemical properties.

Pine nuts are a famous food in the northeastern part of China. However, pine nut shells (PNSs) are not desirable for consumers and they are discarded as biodegradable waste. From this perspective, PNSs are an ideal precursor for preparing hard carbons. In addition, PNSs contain polysaccharides, fat, and lignin. The lignin is beneficial to form amorphous carbon at reasonable carbonization temperatures, which is suitable for our investigation. Herein, we prepare HCs derived from PNSs by repeated washing and thermal processing. The effect of carbonization temperature on the microstructure and Na storage properties of PNSHC-T (T means carbonization temperature) has been investigated by a series of characterization techniques including x-ray diffraction (XRD), scanning electron microscope (SEM), high-resolution transmission electron microscopy (HRTEM), Raman analysis, and electrochemical measurements. It is found that the specific capacity from plateau region for PNSHC-T electrode increases progressively from 144 mAh/g to 220 mAh/g with the increasing carbonization temperature, while the slope capacity demonstrates a downward trend. PNSHC-1400 electrode shows a reversible capacity of ca. 300 mAh/g at 0.1-C rate (where 1 C = 300 mA/g) with a good cycling stability and a high initial coulombic efficiency of 84%.

2. Experimental sections

2.1. Materials preparation

The pine nut shells (purchased in Hei Longjiang province of China) were first washed with deionized water and dried overnight at 100 °C in a drying oven. The dry pine nut shells were then oxidized at 300 °C for 3 hours in a muffle furnace. The oxidized materials were ground into powder and washed with dilute hydrochloric acid and deionized water several times. After filtration and drying, the obtained samples were carbonized at 800 °C for 3 h in a tube furnace under argon flow. Then, a series of repeated washing with dilute hydrochloric acid, concentrated Na hydroxide, and deionized water were carried out. The PNSHC samples were obtained by filtrating and drying. The set of PNSHC-T samples, where T means the carbonization temperature, were produced by directly heating PNSHC samples at 1000 °C, 1200 °C, 1400 °C, and 1600 °C for 3 h under argon environment, respectively.

2.2. Materials characterizations

XRD was carried out with a step of 0.02 degree using a Bruker D8 advance diffractometer equipped with a CuKα radiation ($\lambda_1 = 1.54060$ Å, $\lambda_2 = 1.54439$ Å). The morphologies of the hard carbon materials were investigated using a scanning electron microscope (Hitachi SU-8010). High-resolution transmission electron microscopy images and the corresponding selected area electron diffraction (SAED) patterns were collected by transmission electron microscopy (Tecnai G2 F30) with an accelerating voltage of 300 kV. The global composition was determined with an element analyzer instrument (vario EI cube). The Raman spectra were characterized using a Raman spectroscopy (Renishew inVia).

2.3. Electrochemical measurement

The working electrodes were prepared by mixing 90-wt% active material with 10-wt% Na alginate binder on Cu foil current collectors with the loading mass of the active material ($\sim$ 2 mg/cm^2). The obtained electrodes were dried at 120 °C under vacuum for 8 h and were then fabricated into CR2032 coin-type cells in an argon-filled glove box. Na foils and glass fibers were used as the counter electrodes and the separators, respectively. The electrolyte was a solution of 0.8-mol/L $NaPF_6$ in ethylene (EC) and diethyl carbonate (DEC) (1:1 in volume). The discharge and charge tests were performed at room temperature on a Land BT2000 battery test system (Wuhan, China). Cycling voltammetry measurements were carried out at a scan rate of 0.1 mV/s using an electrochemical workstation (Autolab PG302 N).

3. Results and discussion

The morphologies and particle sizes of PNSHC-T samples are characterized by SEM. All PNSHC-T samples are

composed of blocky-shaped particles with particle sizes in the range of ∼ 3 μm–10 μm. SEM images of PNSHC-1400 are presented in Figs. 1(a) and 1(b). HRTEM and SAED are used to understand the microstructure variation of PNSHC-*T* samples in different carbonization temperatures, as shown in Figs. 1(c)–1(f). As the carbonization temperature increases, the curved graphene layers with random orientation can clearly be observed, indicating the development of graphitic ordering. Meanwhile, the electron diffraction rings become much sharper with the increase of carbonization temperature, further demonstrating the development of an ordered structure.

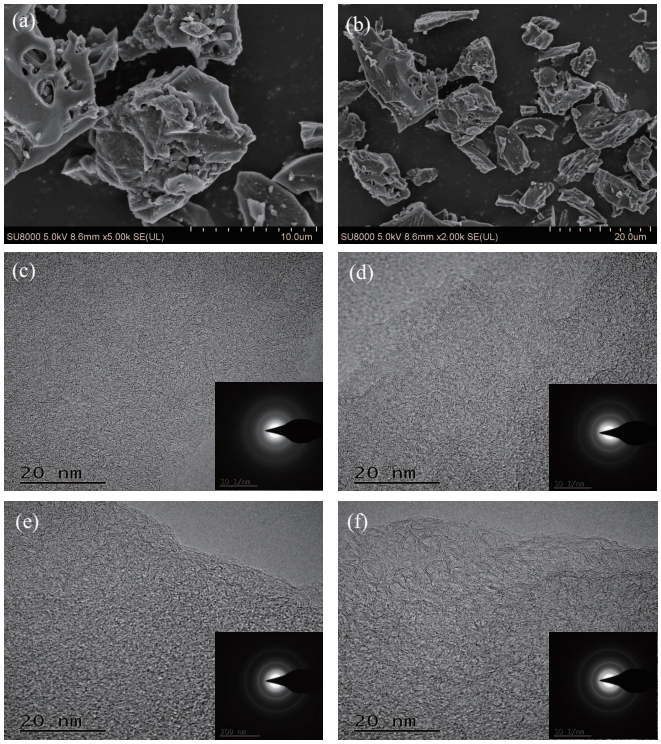


Fig. 1. (a) and (b) SEM pictures of PNSHC-1400. (c)–(f) HRTEM images of PNSHC-1000, PNSHC-1200, PNSHC-1400, and PNSHC-1600, respectively.

XRD patterns (Fig. 2(a)) of all PNSHC-*T* samples show two weak and broad diffraction peaks at about 24° and 43°, corresponding to the (002) and (100) planes of graphite, which is indicative of disordered or amorphous structure. With the increase of carbonization temperature, the (002) diffraction peak shifts to a higher angle. The interplanar spacing $d_{(002)}$ values of PNSHC-1000, PNSHC-1200, PNSHC-1400, and PNSHC-1600 are 0.403 nm, 0.396 nm, 0.388 nm, and 0.372 nm, respectively (Table 1 and Fig. 2(c)). The larger interplanar space of PNSHC-*T* samples is favorable to improve Na ion storage capacity.

Table 1. Physical parameters and electrochemical properties for PNSHC-*T*.

Samples	$d_{(002)}$/nm	I_D/I_G	ICE[a]	Slope /(mAh/g)[b]	Plateau /(mAh/g)[b]
PNSHC-1000	0.403	1.021	78%	116	144
PNSHC-1200	0.396	1.152	81%	109	175
PNSHC-1400	0.388	1.160	84%	89	214
PNSHC-1600	0.372	1.361	85%	67	220

[a]The initial Coulombic efficiency. [b]The slope and plateau capacities are calculated from the second discharge profiles.

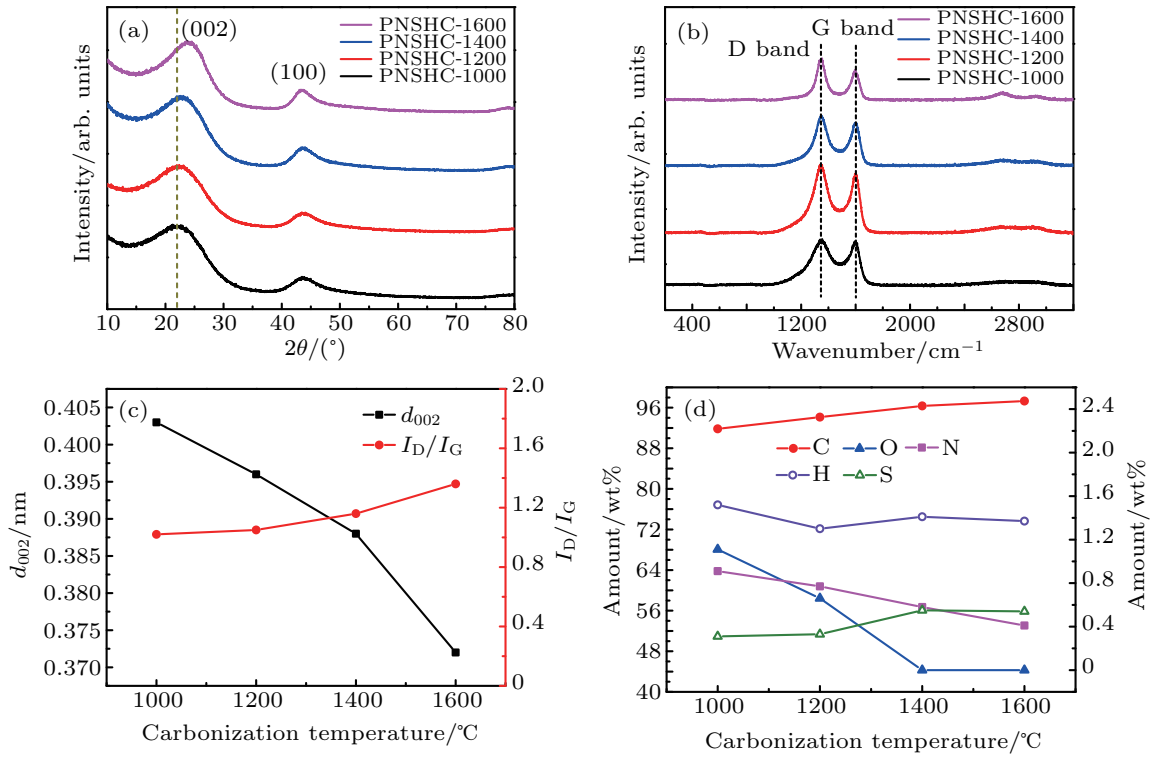


Fig. 2. (a) XRD patterns; (b) Raman spectra of PNSHC-*T* samples; (c) evolution of d_{002} distance and the radio of I_D/I_G; (d) element proportion in PNSHC-*T* samples as a function of temperature.

It can be seen from Fig. 2(b) that all of the samples present two broad bands at ≈ 1359 cm^{-1} (disorder induced D-band) and ≈ 1597 cm^{-1} (in-plane vibrational G-band). Generally, the intensity ratio of D band to G band represents the disorder degree of hard carbon materials. For PNSHC-1000, PNSHC-1200, PNSHC-1400, and PNSHC-1600, the intensity ratios of D band to G band are 1.021, 1.152, 1.160, and 1.361, respectively (Table 1 and Fig. 2(c)), increasing with carbonization temperature. This abnormal trend is attributed to the 300 °C pre-oxidation process, introducing cross-linkage structure, which will lead to the micropore formation during carbonization and induces the more disordered structure.[37] The disordered carbon helps to improve Na's storage performance.

As presented in Fig. 2(d) and Table 2, elemental analysis results of PNSHC-*T* samples show that the increase in temperature leads to a gradual increase of carbon proportion, while the proportion of all other elements shows a downward trend.

The electrochemical behaviors of Na storage in PNSHC-*T* samples are investigated in half coin cells. The cyclic voltammetry curves of PNSHC-1000, PNSHC-1200, PNSHC-1400, and PNSHC-1600 at a scanning rate of 0.1 mV/s between 0 and 2 V are presented in the Figs. 3(a)–3(d). In the initial negative scan, all PNSHC-*T* electrodes show irreversible reduction peaks at about 0.6 V, which disappear at subsequent scans. The irreversible area of PNSHC-*T* electrodes decreases gradually as the carbonization temperature increases, which corresponds to the formation of solid electrolyte interphase (SEI) and the irreversible reaction of electrolyte with surface functional groups. In addition, all PNSHC-*T* electrodes show a pair of sharp redox peaks at about 0.1 V, which is similar to other hard carbon anodes.

Table 2. Proportions of elements in PNSHC-T samples.

Samples	C/%	O/%	N/%	H/%	S/%
PNSHC-1000	91.82	1.11	0.91	1.52	0.31
PNSHC-1200	94.14	0.66	0.77	1.30	0.33
PNSHC-1400	96.34	0	0.58	1.41	0.55
PNSHC-1600	97.3	0	0.41	1.37	0.54

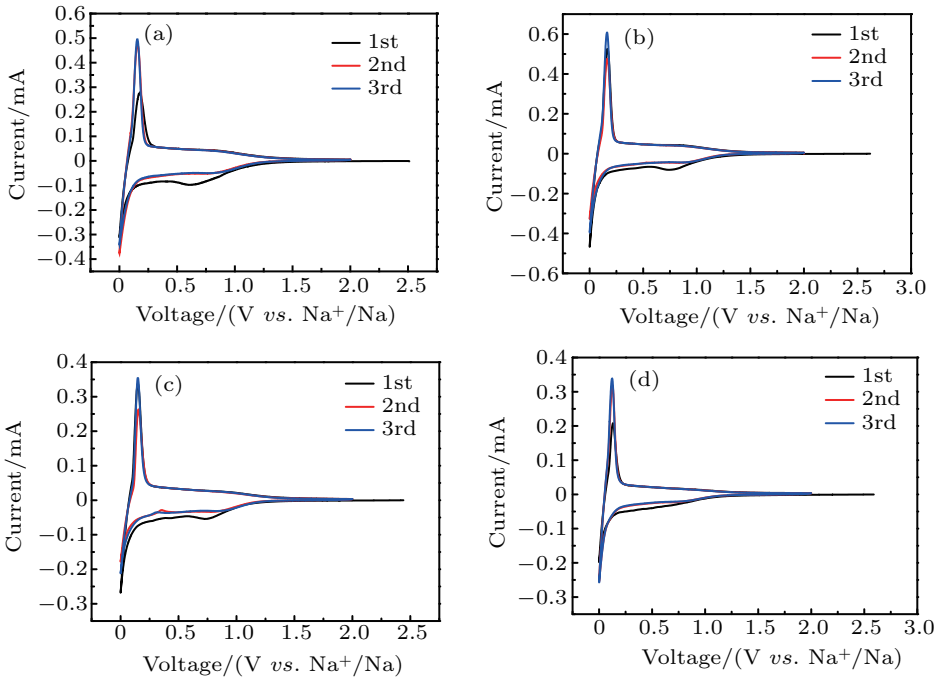


Fig. 3. Cyclic voltammograms (CV) of (a) PNSHC-1000, (b) PNSHC-1200, (c) PNSHC-1400, and (d) PNSHC-1600 electrodes tested at 0.1 mV/s.

The galvanostatic discharge and charge measurements are conducted in the voltage range of 0–2 V *versus* Na^+/Na at 0.1 C. As shown in Fig. 4(a), PNSHC-*T* electrodes exhibit typical voltage profiles including both slope and plateau regions. The reversible capacity for PNSHC-1000, PNSHC-1200, PNSHC-1400, and PNSHC-1600 are 258 mAh/g, 281 mAh/g, 298 mAh/g, and 280 mAh/g, respectively. The initial columbic efficiency of PNSHC-*T* electrodes rises slowly from 78% to 85%.

Calculated from the second cycle curves, as shown in Fig. 5, the specific capacities (Table 1) from the slope regions for PNSHC-1000, PNSHC-1200, PNSHC-1400, and PNSHC-1600 are 116 mAh/g, 109 mAh/g, 89 mAh/g, and 67 mAh/g, respectively. In contrast, the specific capacities from the plateau parts are 144 mAh/g, 175 mAh/g, 214 mAh/g, and 220 mAh/g, respectively, which increase with carbonization temperature.

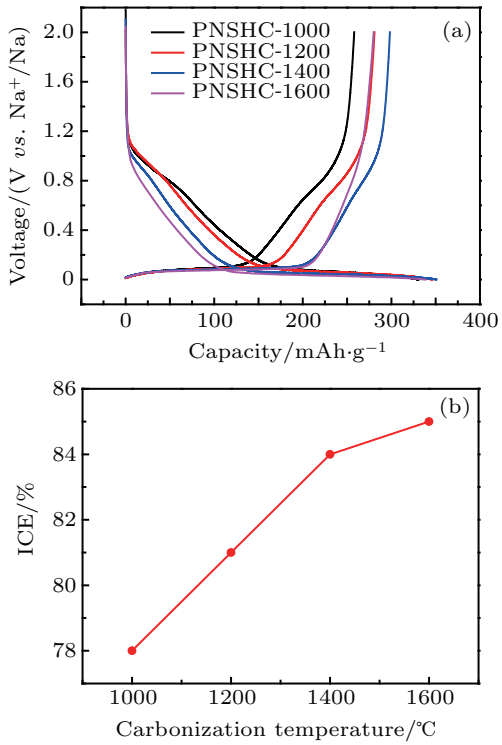


Fig. 4. (a) Voltage profiles and (b) initial Columbic efficiencies of PNSHC-*T* electrodes at 0.1 C rate in the initial cycle.

Rate capabilities of PNSHC-*T* electrodes are tested and shown in Figs. 6(a)–6(d). It is found that the obtained PNSHC-*T* electrodes show moderate rate performance and the specific capacity deteriorates gradually as the charge–discharge current rate increases. For example, the PNSHC-1400 electrode delivers a reversible capacity of 302 mAh/g, 275 mAh/g, 123 mAh/g, 76 mAh/g, and 58 mAh/g at the current rate of 0.1 C, 0.2 C, 0.5 C, 1 C, and 2 C, respectively. The plateau capacity even disappears at high current rates. Hence, the total capacity decay at high rate mainly results from the rapid decay of the plateau capacity.

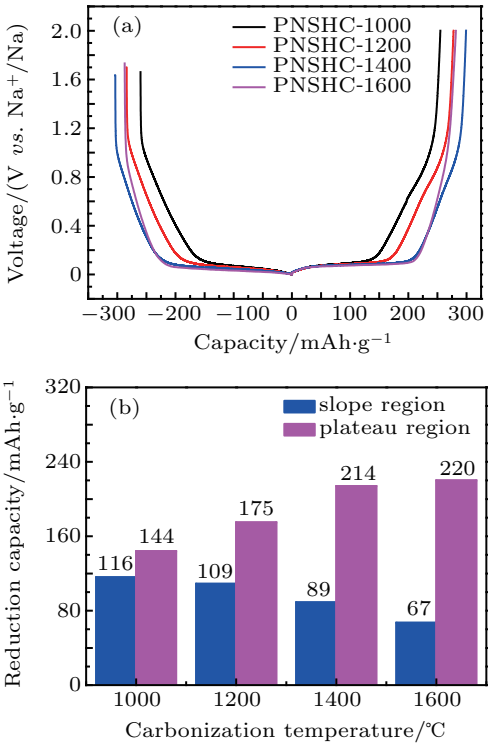


Fig. 5. (a)Voltage profiles and (b) reduction capacities of PNSHC-*T* electrodes at 0.1-C rate in the second cycle.

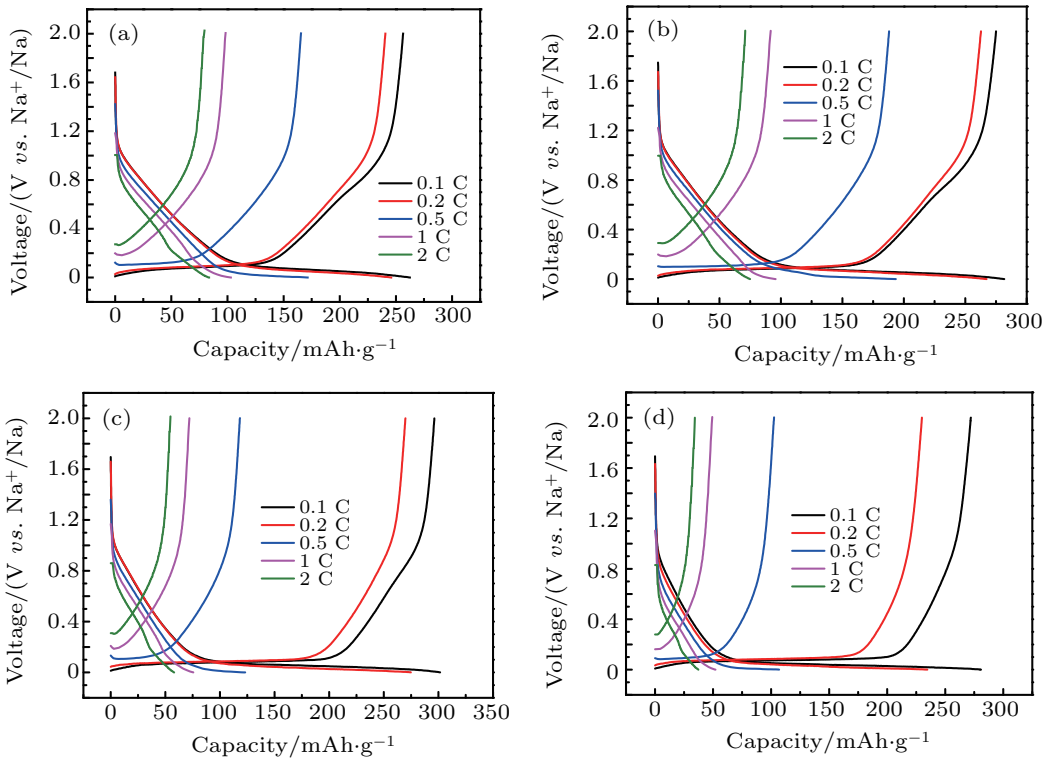


Fig. 6. Rate capabilities of (a) PNSHC-1000, (b) PNSHC-1200, (c) PNSHC-1400, and (d) PNSHC-1600 electrodes.

To further evaluate the cycle stability, PNSHC-1400 is tested at a constant current rate of 0.2 C and the result is shown in Fig. 7. After 100 cycles, PNSHC-1400 electrode retains a reversible capacity of 256 mAh/g, corresponding to a capacity retention of 90%, which demonstrates a good cycle stability. The coulombic efficiency is retained at nearly 99% after the initial cycles.

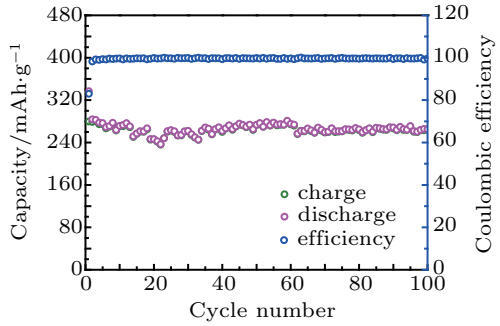


Fig. 7. Cycle performance of PNSHC-1400 electrode at 0.2 C.

4. Conclusion and perspectives

In summary, we have successfully prepared a hard carbon material derived from a biomass waste of pine nut shells by repeated washing and heat treatment procedures. The as-prepared PNSHC-*T* samples are studied as the anodes for NIBs. Among PNSHC-*T* samples, PNSHC-1400 delivers a high reversible capacity of 298 mAh/g at 0.1-C rate with a high initial columbic efficiency of 84%. Meanwhile, it exhibits good cycling stability with a capacity retention of 90% after 100 cycles. Moreover, as the carbonization temperature increases, the plateau capacity of PNSHC-*T* electrode increases progressively from 144 mAh/g to 220 mAh/g, which is very important to high-capacity anode material. We believe that pine nut shells can be used as a potential precursor to prepare hard carbon anodes in NIBs and this work provides some insights into the relationships between synthesis procedures, microstructures, and Na storage properties, which is helpful to design and develop advanced carbon anodes for NIBs.

References

[1] Bruce P G 2008 *Solid State Ion* **179** 752
[2] Goodenough J B and Park K S 2013 *J. Am. Chem. Soc.* **135** 1167
[3] Tarascon J M, Arm and M 2001 *Nature* **414** 359
[4] Palomares V, Serras P, Villaluenga I, Hueso K B, Gonzalez J and Rojo T 2012 *Energy Environ. Sci.* **5** 5884
[5] Palomares V, Cabanas M, Martínez E, Han M H and Rojo T 2013 *Energy Environ. Sci.* **6** 2312
[6] Wang Q, Zhao C, Lu Y, Li Y, Zheng Y, Qi Y, Rong X, Jiang L, Qi X, Shao Y, Pan D, Li B, Hu Y S and Chen L 2017 *Small* **7** 1701835
[7] Kubota K, Yabuuchi N, Yoshida H, Dahbi M and Komaba S 2014 *MRS Bull.* **39** 416
[8] Guo H, Wang Y, Han W, Yu Z, Qi X, Sun K, Hu Y S, Liu Y, Chen D and Chen L 2015 *Electrochim. Acta* **158** 258
[9] Guo G, Wang C, Ming B, Luo S, Su H, Wang B, Zhang M, Yu H J and Wang R Z 2018 *Chin. Phys. B* **27** 118801
[10] Xu S, Wu X, Li Y, Hu Y S and Chen L 2014 *Chin. Phys. B* **23** 118202
[11] Mu L, Hu Y S and Chen L 2015 *Chin. Phys. B* **24** 038202
[12] Wang Y, Xiao R, Hu Y S, Avdeev M and Chen L 2015 *Nat. Commun.* **6** 6954
[13] Jian Z, Zhao L, Pan H, Hu Y S, Li H, Chen W and Chen L 2012 *Electrochem. Commun.* **14** 86
[14] Kawabe Y, Yabuuchi N, Kajiyama M, Fukuhara N, Inamasu T, Okuyama R, Nakai I and Komaba S 2011 *Electrochem. Commun.* **13** 1225
[15] Song W, Ji X, Chen J, Wu Z, Zhu Y, Ye K, Hou H, Jing M and Banks C E 2015 *Phys. Chem. Chem. Phys.* **17** 159
[16] Doeff M M, Ma Y, Visco S J and Jonghe L C 1993 *J. Electrochem. Soc.* **140** 169
[17] Liu Y, Merinov B V and Goddard W A 2016 *Proc. Natl. Acad. Sci.* **113** 3735
[18] Wen Y, He K, Zhu Y J, Han F D, Xu Y H, Matsuda I, Ishii Y, Cumings J and Wang C S 2014 *Nat. Commun.* **5** 4033
[19] Jache B and Adelhelm P 2014 *Angew. Chem. Int. Ed.* **53** 10169
[20] Stevens D A and Dahn J R 2000 *J. Electrochem. Soc.* **147** 1271
[21] Stevens D A and Dahn J R 2001 *J. Electrochem. Soc.* **148** 803
[22] Li Y, Hu Y S, Qi X, Rong X, Li H, Huang X and Chen L 2016 *Energy Storage Mat.* **5** 191
[23] Li Y, Hu Y S, Li H, Chen L and Huang X 2016 *J. Mater. Chem. A* **4** 96
[24] Li Y, Hu Y S, Titirici M M, Chen L and Huang X 2016 *Adv. Energy Mater.* 1600659
[25] Zhao C, Wang Q, Lu Y, Li B, Chen L and Hu Y S 2018 *Sci. Bull.* **63** 1125
[26] Xu S D, Zhao Y, Liu S, Ren X, Chen L, Shi W, Wang X and Zhang D 2018 *J. Mater. Sci.* **53** 12334
[27] Sun N, Liu H and Xu B 2015 *J. Mater. Chem. A* **3** 20560
[28] Lu Y, Zhao C, Qi X, Qi Y, Li H, Huang X, Chen L and Hu Y S 2018 *Adv. Energy Mater.* 1800108
[29] Li Z, Bommier C, Chong Z, Jian Z, Surta T Z, Wang X, Xing Z, Neuefeind J C, Stickle W F, Dolgos M, Greaney P A and Ji X 2017 *Adv. Energy Mater.* 1602894
[30] Li W, Zhou M, Li H, Wang K, Cheng S and Jiang K 2015 *Energy Environ. Sci.* **8** 2916
[31] Wenzel S, Hara T, Janek J and Adelhelm P 2011 *Energy Environ. Sci.* **4** 3342
[32] Tang K, Fu L, White R J, Yu L, Titirici M M, Antonietti M and Maier J 2012 *Adv. Energy Mater.* **2** 873
[33] Cao Y L, Xiao L, Sushko M L, Wang W, Schwenzer B, Xiao J, Nie Z, Saraf L V, Yang Z and Liu J 2012 *Nano Lett.* **12** 3783
[34] Qiu S, Xiao L, Sushko M L, Han K S, Shao Y, Yan M, Liang X, Mai L, Feng J, Cao Y, Ai X, Yang H and Liu J 2017 *Adv. Energy Mater.* **7** 1700403
[35] Bommier C, Surta T W, Dolgos M and Ji X L 2015 *Nano Lett.* **15** 5888
[36] Bai P, He Y, Zou X, Zhao X, Xiong P and Xu Y 2018 *Adv. Energy Mater.* 1703217
[37] Yamamoto H, Muratsubaki S, Kubota K, Fukunishi M, Watanabe H, Kim J and Komaba S 2018 *J. Mater. Chem. A* **6** 16844
[38] Xie X, Kretschmer K, Zhang J, Sun B, Su D and Wang G 2015 *Nano Energy* **13** 208
[39] Qian J, Chen Y, Wu L, Cao Y, Ai X and Yang H 2012 *Chem. Commun.* **48** 7070
[40] Song J, Yu Z, Gordin M L, Hu S, Yi R, Tang D, Walter T, Regula M, Choi D, Li X, Manivannan A and Wang D 2014 *Nano Lett.* **14** 6329
[41] Chen C, Xu H, Zhou T, Guo Z, Chen L, Yan M, Mai L, Hu P, Cheng S, Huang Y and Xie J 2016 *Adv. Energy Mater.* **6** 1600322
[42] Wang Y, Yu X, Xu S, Bai J, Xiao R, Hu Y S, Li H, Yang X, Chen L and Huang X 2013 *Nat. Commun.* **4** 7
[43] Zhao C, Avdeev M, Chen L and Hu Y S 2018 *Angew. Chem. Int. Ed.* **130** 7174
[44] Zhao L, Pan H, Hu Y S, Li H and Chen L 2012 *Chin. Phys. B* **21** 028201
[45] Zhao L, Pan H, Hu Y S, Li H and Chen L 2012 *Chin. Phys. B* **21** 079901
[46] Yu J, Hu Y S, Li H, Huang X and Chen L 2017 *Acta Phys. Sin.* **66** 088201 (in Chinese)